Dynamic Fracture Toughness of Polypropylene Reinforced with Cellulose Fiber

Craig M. Clemons, USDA Forest Service, Forest Products Laboratory [a]
A. Jeffrey Giacomin, University of Wisconsin

Abstract

To better understand mechanisms of fracture under impact loading in cellulose-reinforced polypropylene, dynamic fracture analysis was performed based on linear elastic fracture mechanics. Dynamic critical energy release rates and dynamic critical stress intensity factors were deduced from data obtained from instrumented Charpy impact test measurements. Dynamic fracture toughness was found to increase with cellulose content. However, the assumption of linear elasticity began to break down at a cellulose fiber content of 40%. Scanning electron microscopy showed considerable fiber curl in composites, especiatly at low fiber contents; at high fiber contents, composites developed a three-layer structure.

Introduction

Natural fibers offer an attractive reinforcement for low melt temperature thermoplastics. These fibers represent low cost, renewable reinforcements that increase such mechanical properties as stiffness, strength, and heat deflection under load when added to thermoplastics. In addition, natural fibers are lighter, less abrasive, and often cheaper than conventional inorganic fillers and reinforcements.

To optimize the mechanical performance of composites made with natrual fibers, it is necessary to understand microstructure—property relationships. Work at the Forest Products Laboratory (FPL), USDA Forest Service, currently centers around the impact performance of these composites. To better understand the mechanisms of fracture in the composites under impact loading, a dynamic fracture analysis was performed on Charpy impact test results.

Experimental

The polymer Fortilene 1602, a 12-g/10-min melt flow index (MFI) polypropylene homopolymer (Solvay Polymers, Inc. Deer Park, TX[b]), was chosen for maintaining consistency in the FPL research program and because a high MFI polymer was necessary to offset the dramatic increase in viscosity with the addition of reinforcing fiber. The dissolving pulp fiber, Ultranier-J (Rayonier, Stamford, CT), a bleached chemical pulp, was chosen as a model cellulosic reinforcing fiber because of its high purity and relatively high aspect ratio and fiber length. This pulp fiber was supplied in pressed and dried sheets.

The polypropylene and cellulosic fiber were compounded in a l-L high-intensity thermokinetic mixer (K Mixer, Synergistics, Inc, Ste. Remi de Napierville, Quebec), a simple batch mixer by which several high-speed blades supply the energy to melt the polymer and blend the materials. The temperature of the material is monitored by an infrared sensor. The material is discharged at a set temperature, cooled in a cold press, and granulated. Batches of 150 g were processed at 5000 rpm (rotor tip speed of 32.9 m/s) with discharge temperatures from 180°C to 210°C, depending on the cellulose fiber loading. Resulting batch times ranged from 30 to 60 s. It was necessary to vary the processing conditions to ensure proper dispersion and to allow proper discharge.

The compounded material was dried at 105°C for at least 4 h before injection molding with a 33-t reciprocating screw injection molding machine (Cincinnati Milacron, Batavia, Ohio). Barrel temperatures were kept below 200°C and mold temperature was 40°C. Injection speeds and pressures necessarily varied with the different materials and material viscosities.

Type I tensile specimens were molded in a standard mold and tested using an MTS universal testing machine at 5 mm/min following ASTM D-638 (1). Plaques measuring 76 by 127 by 6.4 mm were molded for impact testing. Longitudinal and transverse specimens measuring 63.5 by 12.7 by 6.4 mm were cut from the plaques, notched with a fly cutter (V-notch, 45° angle) to the desired depth, and sawn with a razor blade to produce a sharp crack.

Specimens were tested at 1 m/s on a Dynatup GRC 8250 instrumented impact tester (gravity-driven) using a Charpy jig with a 51-mm span (GRC Instruments, Munroeville, PA). The linear elastic fracture analysis of Plati and Williams (2) was used to evaluate dynamic fracture toughness. For evaluation of dynamic critical stress intensity factors (K_c), the following equation was used:

$$\sigma Y = K_c (a)^{-1/2} \qquad [1]$$

where σ is maximum gross bending stress, Y the

[a] The Forest Products Laboratory is maintained in cooperation with the University of Wisconsin. This article was written and prepared by U.S. Government employees on official time, and it is therefore in the public domain and not subject to copyright.

The use of tradenames is for reader information only and does not apply endorsement by the U.S. Department of Agriculture of any product or service.

calibration factor, and a crack length. For evaluating the dynamic critical energy release rate (G_c),

$$w = G_c BD\phi \quad [2]$$

where w is energy to maximum stress, B specimen thickness, D specimen width, and ϕ the calibration factor.

Specimens with various crack depths were tested and fracture toughness parameters were determined from the slopes of plots of σY versus $(a)^{-1/2}$ for K_c and w versus $DB\sigma$ for G_c. Both Y and σ are calibration factors that are functions of crack length and geometry and have been determined elsewhere (3).

The intercepts of the plots are generally considered to result from inertial effects associated with the acceleration of the specimen. The theoretical values of these effects can be calculated using the equation of Plati and Williams (2):

$$k_e = (1 + e)\,[1 + m(1 - e)/2\,M]m[M/(m + M)]V^2 \quad [3]$$

where k_e is correction for inertial effects, e coefficient of restitution, m mass of specimen, M mass of impactor, and V velocity of impactor. Since $m << M$, the above equation reduces to

$$k_e = (1 + e)mV^2 \quad [4]$$

Also, an f ratio can be calculated as a check against the domination of kinetic energy effects (3). It is defined as the ratio of absorbed energy $(G_c BD\sigma)$ divided by the upper bound kinetic energy $2mV2$ or

$$f = G_c\phi/2L\rho V^2 \quad [5]$$

where G_c is critical energy release rate, ϕ a calibration factor, L total length of specimen, and ρ material density.

Fractured specimens were mounted on a sample holder with silver paste and sputtered with gold at 40 kV for 2 min. Samples were then analyzed on a Jeol JSM-840 scanning microscope.

Results and Discussion

Microscopy

Scanning electron microscrographs (SEMs) of the fracture surfaces showed a large amount of fiber pullout. This is not surprising because of the lack of compatibility between the two components.

Composite samples containing higher cellulose fiber contents showed a layered structure similar to that of injection-molded inorganic fiber reinforced thermoplastics described by others (4,5), Fibers near the outer surfaces of the plaques were oriented in the filling direction because of shear through the thickness of the plaque as the mold was filled (Fig. 1). The central region of the plaque was the last to solidify and bore the brunt of the high packing pressures during molding, which can cause the fibers to orient more perpendicular to the flow direction (Fig. 2). This morphology was most obvious in the composite samples with higher fiber content. The degree of orientation decreased rapidly as the cellulose fiber content was decreascd.

The SEMs of microtomed sections showed considerable fiber curvature or curl in the composite sample, particularly at low fiber levels. This relatively large fiber curl must be kept in mind when discussing fiber orientation issues. Although a general fiber direction may be identified, significant local deviation from this orientation arises.

Mechanical Testing

The tensile curves to maximum load are shown in Figure 3. These curves are typical of fiber-reinforced polypropylene. An increase in cellulose fiber resulted in increase in modulus but a reduction in strain to maximum load (i.e., a stiffer but more brittle composite). Also despite the chemical incompatibility of the cellulose fiber and the polypropylene matrix, the maximum load increased with cellulose fiber content as more of the applied stress is transferred to the stronger cellulose fibers. Greater improvements in tensile strength of similar composites have been shown with addition of compatibilizers, especially 10 maleated polypropylenes (6). Unfortunately, an increase in compatibility often results in fiber breakage, which typically dissipates less applied energy than does fiber pullout and can result in lower fracture toughness (7).

In our study, the focus of the mechanical testing was the fracture mechanics analysis of Charpy impact tests. A fracture mechanics analysis was used to remove the geometry dependence of the test results and to more closely examine the performance of the material itself. Energy and stress analyses were performed on the raw data. Despite its inherent difficulties (kinetic effects, vibrational problems of test fixture), dynamic fracture toughness was investigated because impact performance has been one shortcoming of thermoplastics reinforced with natural fibers and has therefore been under considerable investigation in our research program. The Charpy configuration was chosen because it is an often measured property, it does not have the further complication of grip tightness as does the Izod test, and it is effectively a dynamic version of the single-edge notch plate in bending configuration, a common specimen configuration in fracture mechanics testing of thermoplastics.

At an impactor speed of 1 m/s, most composite samples exhibited brittle, linear elastic behavior with almost all the energy used in crack initiation rather than propagation. However, significant deviation from that behavior began around a fiber level of 40% by weight where the load versus deflection curve began began to bend.

Yield stress and energy to maximum load were used for

4 and 5 show typical plots whose slopes are G_c and K_c, respectively; Table 1 summarizes the dynamic toughness data and sample coefficient of determination values (r^2) obtained by linear regression.

In general, the data fail on straight lines, indicating the validity of the assumption of linear elasticity. However, at 40% cellulose fiber loading, the plots show some degree of curvature. In unfilled polymers, curvature is usually attributed to yielding of the polymer, resulting in delocalization of the stress concentration at the crack tip. For unlined polymers, a confection is usually applied by approximating the plastic zone size and adding it to the crack length. However, it seems unlikely that increased plastic yielding is occurring at higher cellulose fiber contents. In fact, the converse is usually true, as shown by the embrittlement in the tensile curves with increase in cellulose fiber content. Delocalization of the stress state may have occurred as a result of the cellulose fibers; that is, the transfer of stresses to fibers expanded the stress zone at the crack tip. This would particularly be the case at higher fiber contents. Also, energy-dissipating mechanisms within the cellulose fibers themselves may contribute to a greater extent in the composite samples with higher fiber content. As a first-order approximation for the 40% blends, the slope was conservatively estimated as the slope from a least square fit.

Positive intercepts of plots such as those in Figures 4 and 5 have been shown to be caused by inertial effects associated with acceleration of the specimen. This intercept can be calculated with Equation [4]. Because of the high impactor-to-specimen ratio and the small mass and moderate test speed, the intercepts were nearly zero. As a further check, f ratios were calculated using Equation [5] (see Table 1), This ratio was proposed by Plati and Williams (3) to compare absorbed energy to calculated upper bound inertial energy. F must be at least 0.5 for inertial energy effects not to interfere with measurement of G_c. The high ratios seen in the summary table indicate that kinetic energy effects are sufficiently small for accurate determination of fracture toughness.

Both energy and stress analyses (G_c and K_c) showed similar increases in fracture toughness with level of reinforcement (Figs. 6 and 7). The increase in fracture toughness is consistent with reports of other reinforcing fibers in polypropylene (8). The r^2 values show large variability typical of dynamic testing; the low r^2 values for composites with 40% reinforcement reflect the curvature in the ϕY versus $(a)^{-1/2}$ and w versus $DB\ \phi$ plots at high cellulose fiber content. Since G_c values are calculated using total area under the load versus deflection curve rather than just maximum load, G_c is less sensitive to deviations from linear behavior. Hence, the area under load versus deflection curve is less affected by curvature than maximum strength, improved, undoubtedly as a result of fiber orientation. However, the differences were not large, particularly at low cellulose fiber contents. The considerable cud of the cellulose fibers complicates fiber orientation issues. Even if a fiber is nominally oriented in a specific direction, the curvature results in "local orientation" where the fiber may have a different orientation at the point where the crack crosses the fiber. At higher cellulose fiber contents, the fibers are forced to pack themselves more tightly, resulting in greater orientation. Further work on the measurement of fiber orientation and its effect on impact performance is underway.

Conclusions

1. Fiber orientation increases with cellulose fiber content. At high loadings, a material approximating a three-layer structure is formed.
2. The reinforcing fibers can have a high degree of curl in the final composite, Greater curl is seen at lower cellulose fiber contents.
3. Linear elastic fracture mechanics analysis appears to work well for composites with up to about a 30% cellulose fiber content.
4. Both energy and stress analyses show increases in dynamic fracture toughness as level of reinforcement increases. However, G_c and K_c increase fit different rates. This probably reflects different sensitivity to deviations from linear behavior.
5. Transverse specimens show slightly higher dynamic toughness values than do longitudinal specimens (more obvious at higher cellulose fiber contents), but the differences are not great.
6. Kinetic energy effects appear to be quite small with the present experimental setup.

References

1. ASTM D-638-90, American Society for Testing Materials, Annual Standards, 08.01, 1990.
2. Plati, E.; Williams, J.G., *Polymer Engineering and Science* **15**(6):470–477, 1975.
3. Williams J.G., *Fracture Mechanics of Polymers*, Ellis Horwood Limited, West Sussex, England, 1984.
4. Spahr, D.E.; Friedrich, K.; Schultz, J.M.; Bailey, R.S., *Journal of Materials Science* **25**:4427–4439, 1990.
5. Bright, P.F.; Crowson, R.J.; Folkes, M.J., *Journal of Materials Science* **13**:2497, 1978.
6. Sanadi, A.R.; Clemons, C.M.; Rowell, R.; Young, R.A., *Journal of Reinforced Plastics and Composites* **13**(1):54–67, 1994.
7. Clemons, C.M., presented at Woodfiber–Plastics Conference, Madison, WI, May 1995.
8. Friedrich, K., *Composites Science and Technology* **22**:43–74, 1985.

Keywords: Fracture toughness, critical energy release rate, cellulose fiber, polypropylene

Table 1. Dynamic toughness values of polypropylene reinforced with cellulose fiber

CF[a]	Longitudinal specimens				Tangential specimens				Smallest
	G_c		K_c		G_c		K_c		
(%)	kJ/m^2	r^2	MPa•m$^{1/2}$	r^2	kJ/m^2	r^2	MPa•m$^{1/2}$	r^2	f ratio
0	2.35	0.978	3.74	0.963	2.55	0.969	3.71	0.974	6.19
10	2.17	0.969	4.13	0.944	2.69	0.982	4.64	0.970	5.23
20	2.90	0.994	4.87	0.961	2.90	0.995	5.15	0.989	6.13
30	2.87	0.980	5.07	0.961	3.55	0.993	5.59	0.977	5.89
40	3.48	0.943	5.33	0.740	4.62	0.961	6.48	0.831	7.51

[a]Cellulosic reinforcing fiber.

Figure 1. Fracture surface of polypropylene reinforced with 40% cellulose fiber. Outer layer of longitudinal specimen (×200).

Figure 2. Fracture surface of polypropylene reinforced with 40% cellulose fiber. Central layer of longitudinal specimen (×180).

Plastics–Racing into the Future

SOCIETY OF PLASTICS ENGINEERS

VOLUME III—SPECIAL AREAS
1996

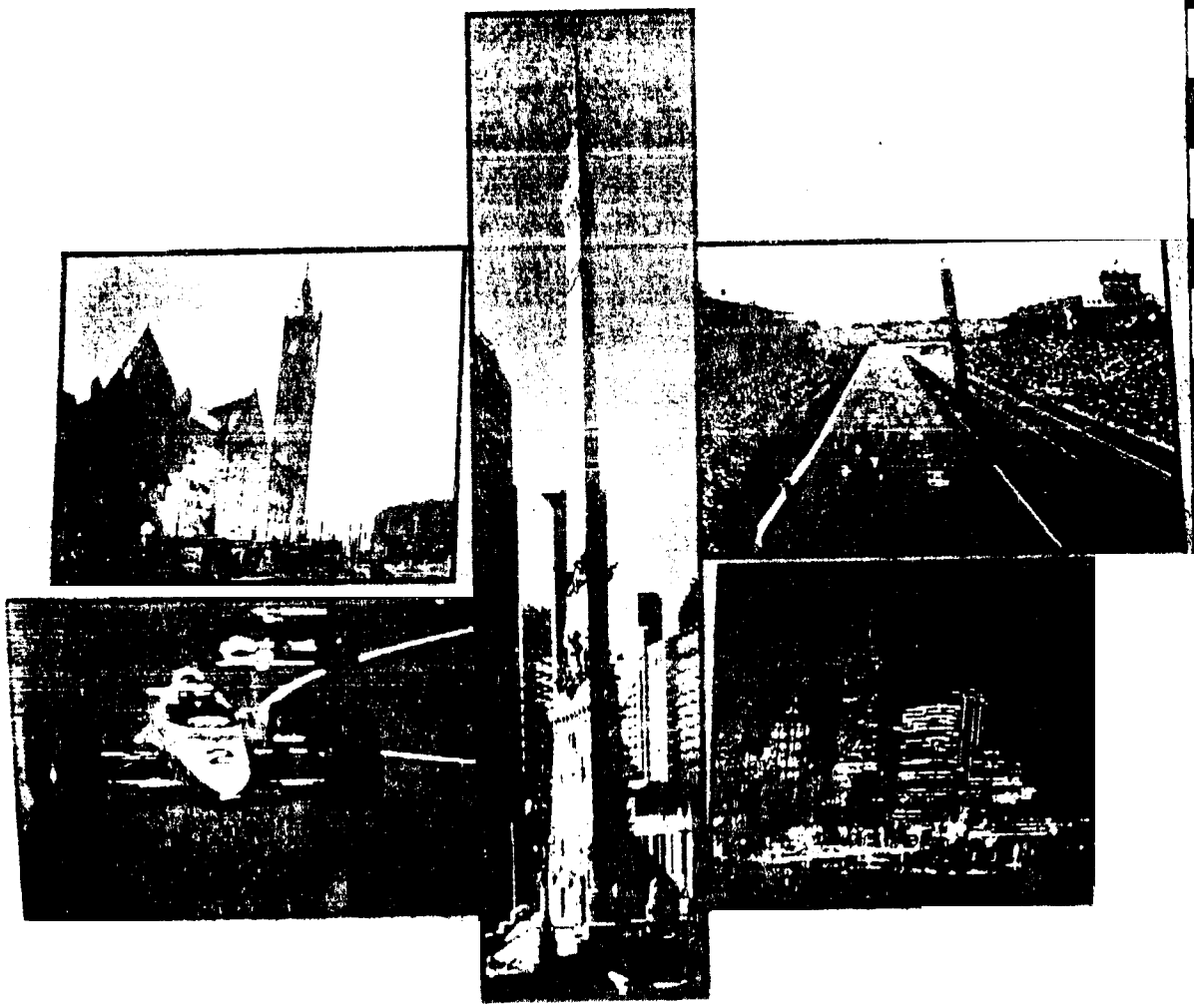

CONFERENCE PROCEEDINGS